

Magnetism and superconductivity in the $t-t'-J$ model

Leonardo Spanu, Massimo Lugas, Federico Becca, and Sandro Sorella

INFN-Democritos, National Simulation Center and International School for Advanced Studies (SISSA), I-34014 Trieste, Italy

(Dated: November 19, 2018)

We present a systematic study of the phase diagram of the $t-t'-J$ model by using the Green's function Monte Carlo (GFMC) technique, implemented within the fixed-node (FN) approximation and a wave function that contains both antiferromagnetic and d-wave pairing. This enables us to study the interplay between these two kinds of order and compare the GFMC results with the ones obtained by the simple variational approach. By using a generalization of the forward-walking technique, we are able to calculate true FN ground-state expectation values of the pair-pair correlation functions. In the case of $t' = 0$, there is a large region with a coexistence of superconductivity and antiferromagnetism, that survives up to $\delta_c \sim 0.10$ for $J/t = 0.2$ and $\delta_c \sim 0.13$ for $J/t = 0.4$. The presence of a finite $t'/t < 0$ induces a strong suppression of both magnetic (with $\delta_c \lesssim 0.03$, for $J/t = 0.2$ and $t'/t = -0.2$) and pairing correlations. In particular, the latter ones are depressed both in the low-doping regime and around $\delta \sim 0.25$, where strong size effects are present.

PACS numbers:

I. INTRODUCTION

After more than twenty years from the discovery of high-temperature superconductivity, a comprehensive description of the cuprate materials is still lacking. One of the main concern is about the origin of the electron pairing, namely if it is due to electron-phonon coupling, like in the standard theory by Bardeen, Cooper and Schrieffer (BCS),¹ or it can be explained by alternative mechanisms, based on the electronic interaction alone. From one side, though the isotope effect in cuprates (if any) is much smaller than the one observed in BCS superconductors, there are experiments suggesting a strong coupling between electrons and localized lattice vibrations.^{2,3} On the other side, besides a clear experimental outcome showing unusual behaviors in both metallic and superconducting phases, there is an increasing theoretical evidence that purely electronic models can indeed sustain a robust pairing, possibly leading to a high critical temperature.^{4,5,6} Within the latter scenario, the minimal microscopic model to describe the low-energy physics has been proposed to be the Hubbard model or its strong-coupling limit, namely the $t-J$ model, which includes an antiferromagnetic coupling between localized spins and a kinetic term for the hole motion.^{7,8} In this respect, Anderson proposed that electron pairing could naturally emerge from doping a Mott insulator, described by a resonating valence bond (RVB) state, where the spins are coupled together forming a liquid of singlets.⁷ Indeed, subsequent numerical calculations for the $t-J$ model,⁹ showed that, though the corresponding Mott insulator (described by the Heisenberg model) has magnetic order, the RVB wave function with d-wave symmetry in the electron pairing can be stabilized in a huge region of doping close to the half-filled insulator. These calculations have been improved by studying the accuracy of such a variational state, giving solid and convincing arguments for the existence of a superconducting phase in the $t-J$ model.⁴ However, other numerical techniques, like

Density Matrix Renormalization Group (DMRG), provided some evidence that charge inhomogeneities can occur at particular filling concentrations.^{10,11} These stripes are probably enhanced by the strong anisotropic boundary conditions used in this approach and can be also found by allowing anisotropies in the hopping and in the super-exchange coupling.¹² Coming back to the projected RVB wave functions, it is worth mentioning that an approximate and simplified description of these states can be obtained by the renormalized mean-field theory (RMFT), the so-called “plain vanilla” approach.¹³ When this approach is applied to the $t-J$ model, it is possible to describe many unusual properties of the high-temperature superconductors and capture the most important aspects of the cuprate phase diagram.¹⁴ However, at present, most of the calculations have been done by neglecting antiferromagnetic correlations, that are definitively important at low doping. Within RMFT and most of the variational calculations, the magnetic correlations are omitted, implying a spin liquid (disordered) state in the insulating regime. Although antiferromagnetism can be easily introduced in both approaches, it is often not satisfactorily described, since the presence of an antiferromagnetic order parameter in the fermionic determinant implies a wrong behavior of the spin properties at small momenta,^{15,16} unless a spin Jastrow factor is used to describe the corresponding spin-wave fluctuations. Indeed, it is now well known that the accurate correlated description of an ordered state is obtained by applying a long-range spin Jastrow factor to a state with magnetic order.^{17,18,19} The important point is that the Gaussian fluctuations induced by the Jastrow term must be orthogonal to the direction of the order parameter, in order to reproduce correctly the low-energy spin-wave excitations. Moreover, by generalizing the variational wave function to consider Pfaffians instead of simple determinants,^{20,21} it is possible to consider both electron pairing and magnetic order, that are definitively important to determine the phase diagram of the $t-J$ model in the low-doping

regime.

The interplay between superconductivity and magnetism is the subject of an intense investigation in the recent years. In most of the thermodynamic measurements these two kinds of order do not coexist, though elastic neutron scattering experiments for underdoped $\text{YBa}_2\text{Cu}_3\text{O}_x$ could suggest a possible coexistence, with a small staggered magnetization.^{22,23,24} On the contrary, in the t - J model, there is an evidence in favor of a coexistence,⁴ the antiferromagnetic order surviving up to a relatively large hole doping, i.e., $\delta \sim 0.1$ for $J/t = 0.2$.²¹ Therefore, the regime of magnetic order predicted by these calculations extend to much larger doping than the experimental results and also the robustness of the coexistence of superconductivity and antiferromagnetism seems to be inconsistent with the experimental outcome. Of course, disorder effects, which are expected to be important especially in the underdoped region, would affect the general phase diagram.²⁵ However, without invoking disorder, one is also interested to understand if alternative ingredients can modify the phase diagram of the simple t - J model. For instance, band structure calculations support the presence of a sizable second-neighbor hopping t' in cuprate materials, showing a possible connection between the value of the highest critical temperature and the ratio t'/t .²⁶ Moreover, an experimental analysis suggests an influence of the value of t'/t on the pseudo-gap energy scale.²⁷ From a theoretical point of view, the effect of t' is still not completely elucidated,^{28,29,30,31,32,33} though there are different calculations providing evidence that a finite t' could suppress superconductivity in the low-doping regime. On the other hand, recent Monte Carlo calculations suggest that the presence of t' (as well as a third-neighbor hopping t'') could induce an enhancement of pairing in optimal and overdoped regions.^{31,32}

In this paper, we want to examine the problem of the interplay between magnetism and superconductivity in the t - J model and its extension including a next-nearest-neighbor hopping t' by using improved variational and Green's function Monte Carlo (GFMC) techniques. Indeed, especially the latter approach has been demonstrated to be very efficient in projecting out a very accurate approximation of the exact ground state and, therefore, can give useful insight into this important issue related to high-temperature superconductivity.

The paper is organized as follows: In Sec. II we describe the methods we used, in Sec. III we show the numerical results for antiferromagnetism and superconductivity, and in Sec. IV we draw our conclusions.

II. MODEL AND METHOD

A. Model and variational wave function

We consider the t - t' - J model on a two-dimensional square lattice with L sites and periodic boundary condi-

tions on both directions:

$$\mathcal{H} = J \sum_{\langle i,j \rangle} \left(\mathbf{S}_i \cdot \mathbf{S}_j - \frac{1}{4} n_i n_j \right) - t \sum_{\langle i,j \rangle \sigma} c_{i,\sigma}^\dagger c_{j,\sigma} - t' \sum_{\langle\langle k,l \rangle\rangle \sigma} c_{k,\sigma}^\dagger c_{l,\sigma} + h.c. \quad (1)$$

where $\langle \dots \rangle$ indicates the nearest-neighbor sites, $\langle\langle \dots \rangle\rangle$ the next-nearest-neighbor sites, $c_{i,\sigma}^\dagger$ ($c_{i,\sigma}$) creates (destroys) an electron with spin σ on the site i , $\mathbf{S}_i = (S_i^x, S_i^y, S_i^z)$ is the spin operator, $S_i^\alpha = \sum_{\sigma,\sigma'} c_{i,\sigma}^\dagger \tau_{\sigma,\sigma'}^\alpha c_{i,\sigma'}$, being τ^α the Pauli matrices, and $n_i = \sum_{\sigma} c_{i,\sigma}^\dagger c_{i,\sigma}$ is the local density operator. In the following, we set $t = 1$ and consider $t' = 0$ and $t'/t = -0.2$. Moreover, we consider two kinds of square clusters: Standard clusters with $L = l \times l$ sites and 45° tilted lattices with $L = 2 \times l^2$ sites. Besides translational symmetries, both of them have all reflection and rotational symmetries.

The variational wave function is defined by:

$$|\Psi_{VMC}\rangle = \mathcal{J}_s \mathcal{J}_d \mathcal{P}_N \mathcal{P}_G |\Phi_{MF}\rangle, \quad (2)$$

where \mathcal{P}_G is the Gutzwiller projector that forbids double occupied sites, \mathcal{P}_N is the projector onto the subspace with fixed number of N particles. Moreover, \mathcal{J}_s is a spin Jastrow factor

$$\mathcal{J}_s = \exp \left(\frac{1}{2} \sum_{i,j} v_{ij} S_i^z S_j^z \right), \quad (3)$$

being v_{ij} variational parameters, and finally \mathcal{J}_d is a density Jastrow factor

$$\mathcal{J}_d = \exp \left(\frac{1}{2} \sum_{i,j} u_{ij} n_i n_j \right), \quad (4)$$

being u_{ij} other variational parameters. The above wave function can be efficiently sampled by standard variational Monte Carlo, by employing a random walk of a configuration $|x\rangle$, defined by the electron positions and their spin components along the z quantization axis. Indeed, in this case, both Jastrow terms are very simple to compute, since they only represent classical weights acting on the configuration.

As previously reported,²¹ the main difference from previous approaches is the presence of the spin Jastrow factor and the choice of the mean-field state $|\Phi_{MF}\rangle$, defined as the ground state of the mean-field Hamiltonian

$$\mathcal{H}_{MF} = \sum_{i,j,\sigma} t_{i,j} c_{i,\sigma}^\dagger c_{j,\sigma} + h.c. - \mu \sum_{i,\sigma} n_{i,\sigma} + \sum_{\langle i,j \rangle} \Delta_{i,j} (c_{i,\uparrow}^\dagger c_{j,\downarrow}^\dagger + c_{j,\uparrow}^\dagger c_{i,\downarrow}^\dagger + h.c.) + \mathcal{H}_{AF}, \quad (5)$$

where we include both BCS pairing $\Delta_{i,j}$ [with d -wave symmetry, i.e., for nearest-neighbor sites $\Delta_k =$

$\Delta(\cos k_x - \cos k_y)$] and staggered magnetic field in the x - y plane

$$\mathcal{H}_{AF} = \Delta_{AF} \sum_i (-1)^{R_i} (c_{i,\uparrow}^\dagger c_{i,\downarrow} + c_{i,\downarrow}^\dagger c_{i,\uparrow}), \quad (6)$$

where Δ_{AF} is a variational parameter that, together with the chemical potential μ and the next-nearest-neighbor hopping of Eq. (5), can be determined by minimizing the variational energy of \mathcal{H} . Whenever both Δ and Δ_{AF} are finite, the projection $\langle x | \Phi_{MF} \rangle$ of the mean-field state on a given configuration $|x\rangle$ can be described in terms of Pfaffians, instead if $\Delta = 0$ or $\Delta_{AF} = 0$ it can be described by using determinants. Moreover, only in the case where the magnetic order parameter is in the x - y plane, the presence of the spin Jastrow factor (3) can introduce relevant fluctuations over the mean-field order parameter Δ_{AF} , leading to an accurate description of the spin properties. A detailed description of the wave function of Eq. (2) and its physical properties can be found in Ref. 21. The variational parameters contained in the mean-field Hamiltonian (5) and in the Jastrow factors (3) and (4) are calculated by using the optimization technique described in Ref. 34, that makes it possible to handle with a rather large number of variational parameters.

B. GFMC: beyond the Variational Monte Carlo

The optimized variational wave function $|\Psi_{VMC}\rangle$ can be also used within the GFMC method to filter out an approximation of the ground state $|\Psi_0^{FN}\rangle$. Indeed, due to the presence of the fermionic sign problem, in order to have a stable numerical calculation, the GFMC must be implemented within the fixed-node (FN) approach, that imposes to $|\Psi_0^{FN}\rangle$ to have the same nodal structure of the variational ansatz.³⁵ Here, we recall the basic definitions of the standard FN method. A detailed description of this technique can be found in Ref. 21.

Starting from the original Hamiltonian \mathcal{H} , we define an effective model by

$$\mathcal{H}_{eff} = \mathcal{H} + O. \quad (7)$$

The operator O is defined through its matrix elements and depends upon a given *guiding* function $|\Psi\rangle$, that is for instance the variational state itself, i.e., $|\Psi_{VMC}\rangle$:

$$O_{x',x} = \begin{cases} -\mathcal{H}_{x',x} & \text{if } s_{x',x} = \Psi_{x'} \mathcal{H}_{x',x} \Psi_x > 0 \\ \sum_{y, s_{y,x} > 0} \mathcal{H}_{y,x} \frac{\Psi_y}{\Psi_x} & \text{for } x' = x, \end{cases}$$

where $\Psi_x = \langle x | \Psi \rangle$, $|x\rangle$ being an electron configuration with definite z -component of the spin. Notice that the above operator annihilates the guiding function, namely $O|\Psi\rangle = 0$. Therefore, whenever the guiding function is close to the exact ground state of \mathcal{H} , the perturbation O is expected to be small and the effective Hamiltonian becomes very close to the original one. The most important property of this effective Hamiltonian is that its

ground state $|\Psi_0^{FN}\rangle$ can be efficiently computed by using GFMC.^{36,37} The distribution $\Pi_x \propto \langle x | \Psi \rangle \langle x | \Psi_0^{FN} \rangle$ is sampled by means of a statistical implementation of the power method: $\Pi \propto \lim_{n \rightarrow \infty} G^n \Pi^0$, where Π^0 is a starting distribution and $G_{x',x} = \Psi_{x'} (\Lambda \delta_{x',x} - \mathcal{H}_{eff,x',x}) / \Psi_x$, is the so-called Green's function, $\delta_{x',x}$ being the Kronecker symbol. The statistical method is very efficient since all the matrix elements of G are non-negative and, therefore, G can represent a transition probability in configuration space, apart for a normalization factor $b_x = \sum_{x'} G_{x',x}$. Since $|\Psi_0^{FN}\rangle$ is an exact eigenstate of the effective Hamiltonian \mathcal{H}_{eff} , the corresponding ground-state energy can be evaluated efficiently by computing

$$E_{MA} = \frac{\langle \Psi_{VMC} | \mathcal{H}_{eff} | \Psi_0^{FN} \rangle}{\langle \Psi_{VMC} | \Psi_0^{FN} \rangle}, \quad (8)$$

namely the statistical average of the local energy $e_L(x) = \langle \Psi_{VMC} | \mathcal{H} | x \rangle / \langle \Psi_{VMC} | x \rangle$ over the distribution Π_x . The quantity $E_{MA} \leq E_{VMC}$ because, by the variational principle $E_{MA} \leq \langle \Psi | \mathcal{H}_{eff} | \Psi \rangle / \langle \Psi | \Psi \rangle = E_{VMC}$. Moreover, E_{MA} represents an upper bound of the expectation value E_{FN} of \mathcal{H} over $|\Psi_0^{FN}\rangle$, as it is shown in Ref. 35 or it can be simply derived by considering that the operator O is semi-positive definite, namely all its eigenvalues are non-negative. In the following, we will denote by FN the (variational) results obtained by using the GFMC method with fixed-node approximation, whereas the standard variational Monte Carlo results obtained by considering the wave function of Eq. (2) will be denoted by VMC.

Summarizing the FN approach is a more general and powerful variational method than the straightforward variational Monte Carlo. Within the FN method, the wave function $|\Psi_0^{FN}\rangle$, the ground state of \mathcal{H}^{eff} is known only statistically, and, just as in the variational approach, E_{FN} depends explicitly on the variational parameters defining the guiding function $|\Psi\rangle$. This is due to the fact that \mathcal{H}_{eff} depends upon $|\Psi\rangle$ through the operator O . The main advantage of the FN approach is that it provides the exact ground-state wave function for the undoped insulator (where the signs of the exact ground state are known), and therefore it is expected to be particularly accurate in the important low-doping region. Moreover, the FN method is known to be very efficient in various cases: For instance, it has allowed to obtain a basically exact description of the three-dimensional system of electrons interacting through the realistic Coulomb potential (in presence of a uniform positive background).³⁸ Therefore, it represents a very powerful tool to describe correlated electronic systems.

III. RESULTS

A. Phase separation

Before showing the results on magnetic and superconducting properties, we briefly discuss the stability against

phase separation. In order to detect a possible phase separation, it is very useful to follow the criterion given in Ref. 39 and consider the energy per hole:

$$e_h(\delta) = \frac{e(\delta) - e(0)}{\delta}, \quad (9)$$

where $e(\delta)$ is the energy per site at hole doping δ and $e(0)$ is its value at half filling. In practice, $e_h(\delta)$ represents the chord joining the energy per site at half filling and the one at doping δ . For a stable system, $e_h(\delta)$ must be a monotonically increasing function of δ , because the ground-state energy of a short-range Hamiltonian is a convex function of the doping. By performing exact energy calculations on finite clusters, the phase separation instability is marked by a minimum of $e_h(\delta)$ at a given δ_c and by a flat behavior up to δ_c in the thermodynamic limit. For an approximate variational technique based on a spatially homogeneous ansatz, this flat behavior is never reached in the phase separated region, so that $e_h(\delta)$ remains with a well defined minimum even for very large sizes; in this case, δ_c can be estimated with the Maxwell construction, provided the variational ansatz is accurate enough. In Ref. 21, we demonstrated the existence of an homogeneous state for $t' = 0$ and $J/t \lesssim 0.7$. As shown in Table I, the FN approximation, that is exact at zero doping,²¹ provides a substantial lowering of the VMC energy, especially away from half filling and for a finite t' . This is a first indication that, for $t'/t < 0$, the simple variational approach could not be adequate to provide a reliable quantitative description of the ground-state properties.

The FN results clearly indicate that the inclusion of a negative next-nearest-neighbor hopping contributes to further stabilize the homogeneous phase at finite doping, see Fig. 1. This result is compatible with the outcome of recent calculations based on cluster dynamical mean-field theory on the Hubbard model, where a negative ratio t'/t enhances the stability of the homogeneous phase, whereas positive values of t' favor phase separation.⁴⁰ In this work, we do not want to address in much detail this issue and we will focus our attention on the more interesting magnetic and superconducting properties.

B. Antiferromagnetic properties

Here we present the results for the magnetic properties of the $t-t'-J$ model and compare the FN approach with the VMC one, based upon the wave function (2). As already discussed in Ref. 21, the optimized wave function (2) breaks the $SU(2)$ spin symmetry, because of the magnetic order parameter Δ_{AF} of Eq. (6) and the spin Jastrow factor (3). It turns out that at half-filling and in the low-doping regime, the variational state (2) has an antiferromagnetic order in the $x-y$ plane, whereas the spin-spin correlations in the z axis decay very rapidly. Therefore, in order to assess the magnetic order at the

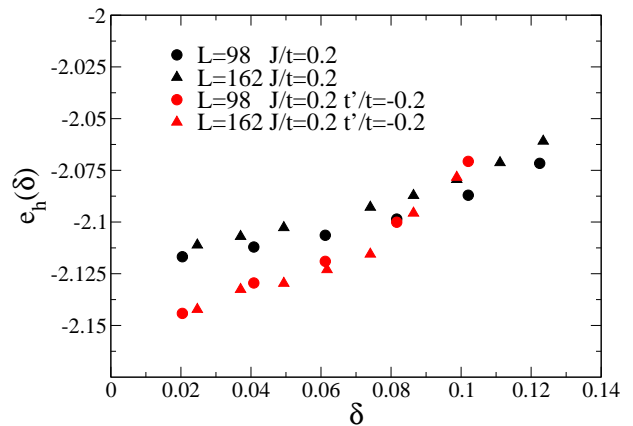


FIG. 1: (Color online) Energy per hole $e_h(\delta)$, calculated by using the FN method, as a function of the doping δ for $L = 98$ and 162 and two values of the next-nearest-neighbor hopping $t'/t = 0$ and -0.2 .

TABLE I: Variational (VMC) and fixed-node (FN) energies per site for $J/t = 0.2$ and $t' = 0$ (third and fourth columns), and $t'/t = -0.2$ (fifth and sixth columns) for two clusters with $L = 98$ and 162 and different hole concentrations $N_h = L - N$

L	N_h	E_{VMC}/L	E_{FN}/L	E_{VMC}/L	E_{FN}/L
98	0	-0.233879(1)	-0.23432(1)	-0.233879(1)	-0.23432(1)
98	2	-0.274144(5)	-0.27752(1)	-0.27290(1)	-0.27808(1)
98	4	-0.31429(1)	-0.32053(1)	-0.31189(1)	-0.32123(1)
98	6	-0.35482(1)	-0.36328(1)	-0.35132(1)	-0.36405(1)
98	8	-0.39550(1)	-0.40563(2)	-0.39028(1)	-0.40575(1)
98	10	-0.43581(1)	-0.44728(2)	-0.42814(1)	-0.44561(1)
162	0	-0.233707(1)	-0.23409(1)	-0.233707(1)	-0.23409(1)
162	2	-0.258002(5)	-0.26020(1)	-0.257260(5)	-0.26012(1)
162	4	-0.282117(5)	-0.28621(1)	-0.28067(1)	-0.28698(1)
162	6	-0.306324(5)	-0.31212(1)	-0.30429(1)	-0.31307(1)
162	8	-0.33060(1)	-0.33793(1)	-0.32807(1)	-0.33925(2)
162	10	-0.35498(1)	-0.36360(2)	-0.35207(1)	-0.36514(2)
162	12	-0.37954(1)	-0.38912(2)	-0.37567(1)	-0.39079(2)
162	14	-0.40406(1)	-0.41446(2)	-0.39939(1)	-0.41520(2)
162	16	-0.42838(1)	-0.43946(2)	-0.42232(1)	-0.43936(2)

variational level, we have to consider the isotropic spin-spin correlations:

$$\langle \mathbf{S}_0 \cdot \mathbf{S}_r \rangle = \frac{\langle \Psi_{VMC} | \mathbf{S}_0 \cdot \mathbf{S}_r | \Psi_{VMC} \rangle}{\langle \Psi_{VMC} | \Psi_{VMC} \rangle}. \quad (10)$$

The FN approach alleviates the anisotropy between the $x-y$ plane and the z axis; in this case, we find that a rather accurate (and much less computational expensive) way to estimate the magnetic moment can be obtained from the z component of the spin-spin correlations:

$$\langle S_0^z S_r^z \rangle = \frac{\langle \Psi_0^{FN} | S_0^z S_r^z | \Psi_0^{FN} \rangle}{\langle \Psi_0^{FN} | \Psi_0^{FN} \rangle}. \quad (11)$$

This quantity can be easily computed within the forward-walking technique,³⁷ because the operator $S_0^z S_r^z$ is diagonal in the basis of configurations used in the Monte Carlo

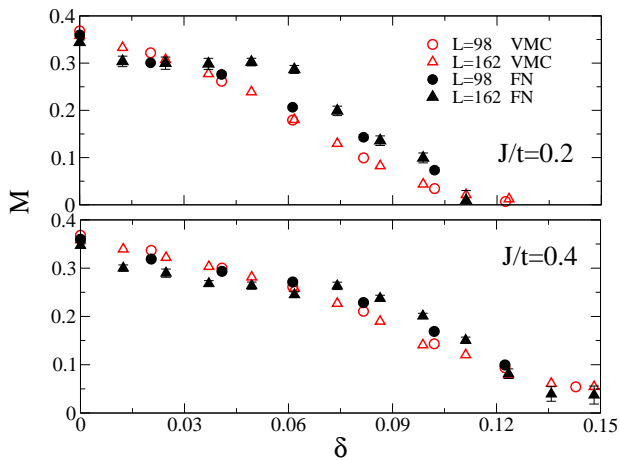


FIG. 2: (Color online) Magnetization obtained from the spin-spin correlations at the maximum distance calculated for the t - J model with $J/t = 0.2$ (upper panel) and $J/t = 0.4$ (lower panel). For the VMC calculations the error-bars are smaller than the symbol sizes. The VMC magnetization has been obtained from the isotropic correlations, whereas the FN one from the correlations along the z axis (see text).

sampling. From the spin-spin correlations at the maximum distance, it is possible to extract the value of the magnetization. In particular, the variational wave function is not a singlet when the antiferromagnetic order sets in, and the magnetization has to be computed with the spin isotropic expression $M = \lim_{r \rightarrow \infty} \sqrt{\langle \mathbf{S}_0 \cdot \mathbf{S}_r \rangle}$. On the other hand, the FN ground state is almost a perfect singlet for all the cases studied and the magnetization can be estimated more efficiently by $M = \lim_{r \rightarrow \infty} \sqrt{3 \langle S_0^z S_r^z \rangle}$. The spin isotropy of the FN wave function can be explicitly checked by computing the mixed-average of the total spin square

$$\langle S^2 \rangle_{MA} = \frac{\langle \Psi_{VMC} | S^2 | \Psi_0^{FN} \rangle}{\langle \Psi_{VMC} | \Psi_0^{FN} \rangle}, \quad (12)$$

that vanishes if $|\Psi_0^{FN}\rangle$ is a perfect singlet, even when $|\Psi_{VMC}\rangle$ has not a well-defined spin value.

In Fig. 2 we report the results of the magnetization in the t - J model with $J/t = 0.2$ and 0.4 . At finite doping, it is not possible to perform a precise size scaling extrapolation since it is very rare to obtain the same doping concentration for different cluster sizes. Moreover, though the FN approach is able to recover an exact singlet state at half filling, $\langle S^2 \rangle_{MA}$ increases by doping, reaching its maximum around $\delta \sim 0.06$, e.g., $\langle S^2 \rangle_{MA} \sim 1$ for 8 holes on 162 sites. This could explain why the FN results are a bit larger than the VMC ones for $\delta \sim 0.06$, especially for $J/t = 0.2$. Definitely, both the VMC and FN wave functions are almost spin singlets close to the transition point, because the mean-field order parameter Δ_{AF} goes to zero together with the parameters defining the spin Jastrow factor. Therefore, we are rather confident in the estimation of the critical doping δ_c , where the

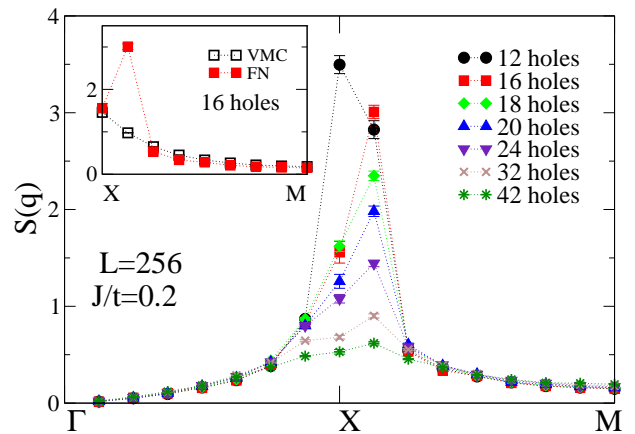


FIG. 3: (Color online) Static spin structure factor $S(q)$ for $L = 16 \times 16$ cluster and different hole concentrations for the t - J model with $J/t = 0.2$. $\Gamma = (0, 0)$, $X = (\pi, \pi)$, and $M = (\pi, 0)$. Inset: $S(q)$ for the variational state (empty symbols) and for the FN approximation (full symbols).

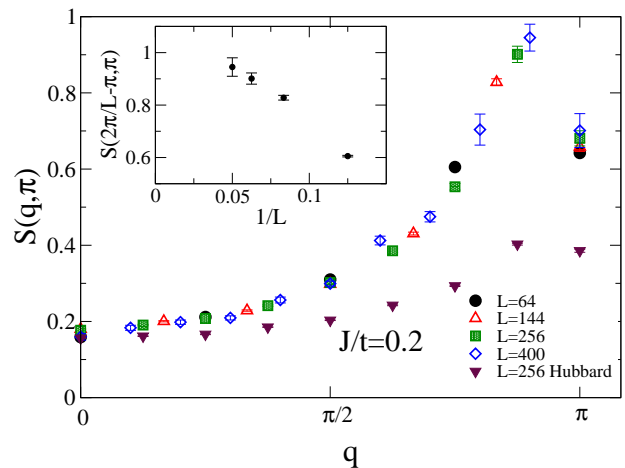


FIG. 4: (Color online) Spin structure factor $S(q)$ for the t - J with $J/t = 0.2$ and doping $\delta = 1/8$ and different clusters ($L = 8 \times 8, 12 \times 12, 16 \times 16$, and 20×20). The case of the Hubbard model at $U/t = 4$ and $L = 16 \times 16$ is also reported for comparison. Inset: Size scaling of the peak as a function of $1/L$.

long-range antiferromagnetic order disappears. In particular, we find $\delta_c = 0.10 \pm 0.01$ and $\delta_c = 0.13 \pm 0.02$ for $J/t = 0.2$ and $J/t = 0.4$, respectively.

At low doping, we have evidence that long-range order is always commensurate, with a (diverging) peak at $X = (\pi, \pi)$ in the static spin structure factor, defined as

$$S(q) = \frac{1}{L} \sum_{l,m} e^{iq(R_l - R_m)} S_l^z S_m^z. \quad (13)$$

This outcome is clear for all kinds of cluster considered, namely both for standard $l \times l$ and 45° tilted lattices. By contrast, close to the critical doping δ_c , we have the indication that some incommensurate peaks develop. Re-

markably, we do not find any strong doping dependence of the peak positions. We show the results of $S(q)$ for the 16×16 cluster and $J/t = 0.2$ in Fig. 3, where the evolution of the peak as a function of the doping δ is reported. By increasing the hole doping, the commensurate peak at X reduces its intensity and eventually the maximum of $S(q)$ shifts to a different k-point, i.e., $(\pi, \pi - 2\pi/L)$. It should be stressed that this outcome is obtained only when the FN projection is applied to the lowest-energy ansatz containing a sizable BCS parameter, and the FN calculation with a fully projected free-electron determinant cannot reproduce an incommensurate peak in $S(q)$. Moreover, the variational wave functions always show commensurate correlations, see inset of Fig. 3. The strong dependence of this feature on the variational ansatz may also indicate that more accurate calculations are necessary to clarify this important aspect of the phase diagram of the $t-J$ model. In order to support the validity and the accuracy of our results, we have applied the same method to the Hubbard model at $U/t = 4$, where essentially exact calculations are available for $S(q)$.⁴¹ In this case, we have reproduced both the position and the intensity of the incommensurate peak on the 10×10 lattice. It is interesting to notice that, within the FN approximation, the intensity of the incommensurate peak at $U/t = 4$ is much smaller than the corresponding one for the $t-J$ model, see Fig. 4. This clearly indicates that in the $t-J$ model the magnetic correlations are much more pronounced than the corresponding ones of the Hubbard model, possibly explaining the origin of the large extension of the antiferromagnetic region found in the $t-J$ model.

We now discuss whether these incommensurate spin correlations remain in the thermodynamic limit. For all the cluster sizes we considered, i.e., up to $L = 20 \times 20$, the incommensurate peak in $S(q)$ always appears at $(\pi, \pi - 2\pi/L)$, namely the closest k-point to X along the border of the Brillouin zone. This indicates that, in the thermodynamic limit, the peak should be located very close to X and it is not compatible with $(\pi, \pi - 2\pi\delta)$, found in cuprate materials.⁴² Although size scaling extrapolations are not possible for a generic hole doping, we do not have evidence that the incommensurate peak diverges, implying no incommensurate long-range order at finite doping concentrations. Nevertheless, once the commensurate magnetic order is melted, the ground state is characterized by short-range incommensurate spin correlations. In Fig. 4, we show the results for $J/t = 0.2$ and $\delta = 1/8$, where different clusters with the same doping are available. Similar calculations with $t'/t = -0.2$ show the same qualitative behavior for the $S(q)$.

Coming back to the commensurate magnetic order close to half-filling, we stress that the pure $t-J$ model shows robust antiferromagnetic correlations, with a critical doping much larger than the one observed in the hole-doped cuprates materials, where the long-range order disappears at $\delta_c \sim 0.05$.⁴² This smaller value of the critical doping cannot be explained by reducing the an-

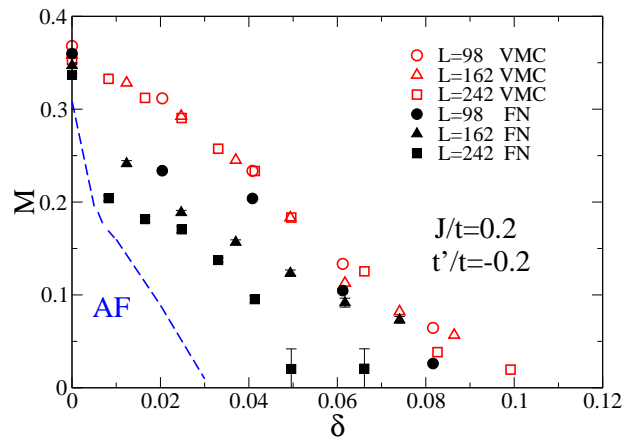


FIG. 5: (Color online) The same as in Fig. 2 for the $t-t'-J$ model with $J/t = 0.2$ and $t'/t = -0.2$. For the VMC calculations the error-bars are smaller than the symbol sizes. The dashed line indicates a tentative estimation for the thermodynamic limit.

tiferromagnetic super-exchange J , given the fact that even for $J/t = 0.2$ we have that $\delta_c \sim 0.1$. Besides disorder effects that can be important in the underdoped regime,²⁵ one important ingredient to be considered in a microscopic model is the next-nearest-neighbor hopping, that was shown to have remarkable effects on both magnetic and superconducting properties.^{28,29,31,32} In particular, in spite exact diagonalization calculations suggest a suppression of antiferromagnetic correlations for negative t'/t ,²⁸ more recent Monte Carlo simulations (also including a further third-neighbor hopping t'') do not confirm these results, pointing instead toward a suppression of superconducting correlations.³²

In Fig. 5, we report the magnetization for $J/t = 0.2$ and $t'/t = -0.2$. The first outcome is that the VMC results, though renormalized with respect to the case $t' = 0$, present a critical doping δ_c which is very similar to the one found for the pure $t-J$ model. By contrast, the FN approach strongly suppresses the spin-spin correlations, even very close to half filling. In this case, the FN results have rather large size effects, that prevent us to extract a reliable estimate for the thermodynamic limit. However, it is clear that the antiferromagnetic region is tiny and we can estimate that $\delta_c \lesssim 0.03$. It should be emphasized that for $t'/t = -0.2$ the variational wave function is not as accurate as for the pure $t-J$ model with $t' = 0$, but nevertheless the projection technique, even if approximate, is able to reduce the bias (e.g., the presence of a large magnetic order up to $\delta \sim 0.1$), showing the importance of alternative numerical methods to assess the actual accuracy of the simple variational approach. Indeed, we are confident that our FN results represent a good approximation of the true ground-state properties. On the contrary, the VMC calculations clearly show that the wave function (2) overestimates the correct value of the magnetic moment.

C. Superconducting properties

In the following, we want to address the problem of the superconducting properties of the Hamiltonian (1). In particular, we would like to obtain an accurate determination of the pair-pair correlations as a function of the hole doping and clarify the role of the next-nearest-neighbor hopping t' . The effect of such term has been recently considered by using different numerical techniques. DMRG calculations for n -leg ladders (with $n = 4$ and 6) showed that the effect of a negative t' is to stabilize a metallic phase, without superconducting correlations.²⁹ Moreover, improved variational Monte Carlo techniques suggested that t' could suppress pairing at low doping, whereas some increasing of superconducting correlations can be found in the optimal doping regime.^{31,32} A further variational study,³⁰ suggested the possibility that a sufficiently large ratio t'/t can disfavor superconductivity and stabilize charge instabilities (stripes) near 1/8 doping.

The pair-pair correlations are defined as

$$\Delta^{\mu,\nu}(r) = S_{r,\mu} S_{0,\nu}^\dagger, \quad (14)$$

where $S_{r,\nu}^\dagger$ creates a singlet pair of electrons in the neighboring sites r and $r + \mu$, namely

$$S_{r,\mu}^\dagger = c_{r,\uparrow}^\dagger c_{r+\mu,\downarrow}^\dagger - c_{r,\downarrow}^\dagger c_{r+\mu,\uparrow}^\dagger. \quad (15)$$

For the first time, we implemented the forward-walking technique in order to compute true expectation values of the pairing correlations over the FN state:

$$\langle \Delta^{\mu,\nu}(r) \rangle = \frac{\langle \Psi_0^{FN} | \Delta^{\mu,\nu}(r) | \Psi_0^{FN} \rangle}{\langle \Psi_0^{FN} | \Psi_0^{FN} \rangle}. \quad (16)$$

Indeed, given the fact that $\Delta^{\mu,\nu}(r)$ is a non-diagonal operator (in the basis of configurations defined before), within the FN approach the previous calculations⁴ were based upon the so-called mixed average, where, similarly to Eqs. (8) and (12), the state on the left is replaced by the variational one. Now, by using Eq. (16), it is possible to verify the fairness of the variational results against a much more accurate estimation of the exact correlation functions given by the FN approach.

The superconducting off-diagonal long-range order implies a non-zero value of $\langle \Delta^{\mu,\nu}(r) \rangle$ at large distance r . In the following, we consider the pair-pair correlation at the maximum distance and $\mu = \nu$ (parallel singlets) both for the VMC and the FN approximations and denote $P_d^2 = 4 \lim_{r \rightarrow \infty} \langle \Delta^{y,y}(r) \rangle$. It is worth noting that, as far as the superconducting correlations are concerned, there is no appreciable difference between the results obtained with and without the antiferromagnetic order parameter and the long-range spin Jastrow factor. The results for the pure t - J model are reported in Fig 6, where we report two different values of the antiferromagnetic coupling, i.e., $J/t = 0.2$ and $J/t = 0.4$. In this case, VMC and FN calculations are in fairly good agreement, giving a similar superconducting phase diagram. Interestingly, the optimal doping, i.e., the doping at which the

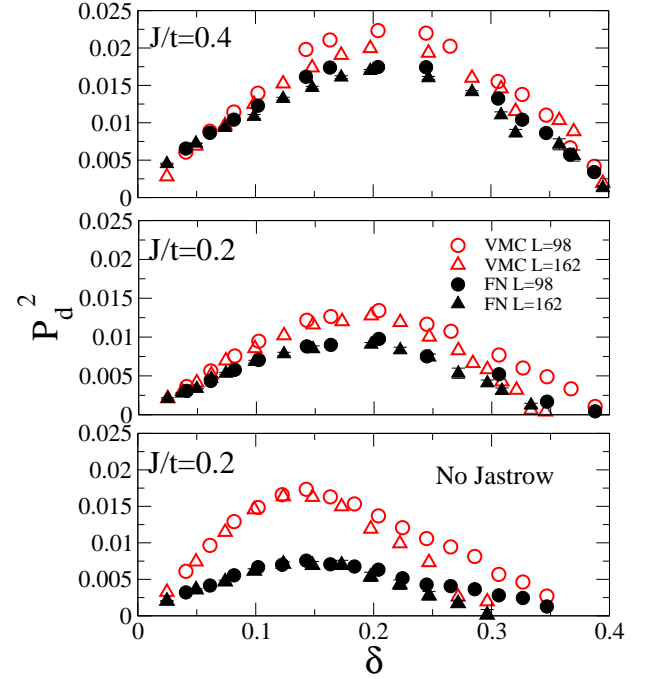


FIG. 6: (Color online) Pair-pair correlations at the maximum distance as a function of the doping for $J/t = 0.4$ (upper panel) and $J/t = 0.2$ (middle panel). The results for the variational wave function (2) (empty symbols) and for the FN approximation (filled symbols) are reported. The results for the wave function without the Jastrow factors (both for spin and density) and magnetic order parameter are also reported (lower panel).

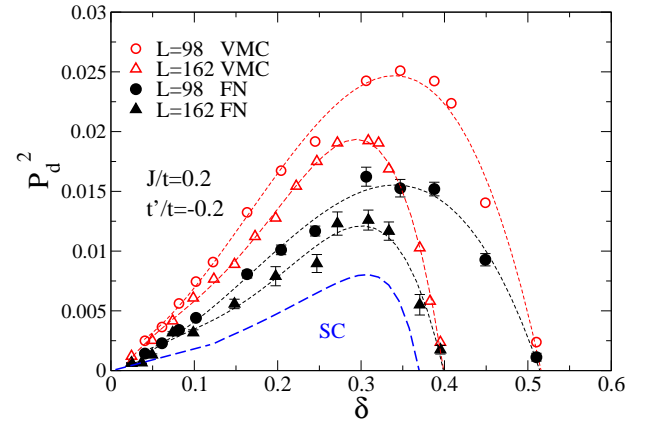


FIG. 7: (Color online) The same as in Fig. 6 for the t - t' - J model with $J/t = 0.2$ and $t'/t = -0.2$. The dashed line indicates a tentative estimation for the thermodynamic limit.

maximum in the pair-pair correlations takes place, occurs in both cases at $\delta \sim 0.2$, whereas the actual value of the correlations is proportional to J/t . At high doping, where antiferromagnetic fluctuations play a minor role, the behavior of the pairing is unchanged when J is varied. Although in this region there are some size effects, we can safely estimate that superconductivity disappears

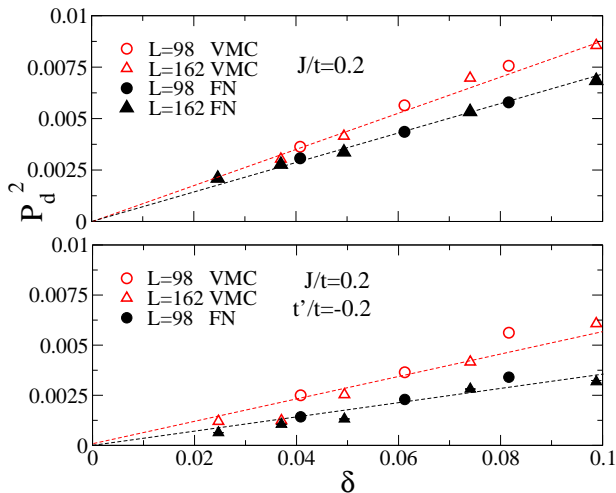


FIG. 8: (Color online) Detail of the pair-pair correlations reported in Figs. 6 and 7 at low doping.

around $\delta \sim 0.35$ and $\delta \sim 0.4$ for $J/t = 0.2$ and $J/t = 0.4$, respectively.

It is worth noting that the density Jastrow term (4) is very important to obtain an accurate estimation of the pairing correlations. Indeed, the variational results, based on the simple wave function with BCS pairing and the on-site Gutzwiller projector (but without the long-range Jastrow factors) overestimate the pairing correlations at optimal doping by at least a factor two. Remarkably, the FN approach is able to correct this bias, providing approximately the same results as the one obtained starting from the wave function with the long-range Jastrow factor, see Fig. 6. This fact shows that the FN method is particularly reliable for estimating the pairing correlations.

The inclusion of the next-nearest-neighbor hopping induces sizable modifications in the pairing correlations, though the qualitative dome-like behavior remains unchanged, see Fig. 7. At low doping there is a sizable suppression of the superconducting pairing, particularly evident after the FN projection, see Fig. 8. Indeed, while for the pure t - J model we clearly obtain a linear behavior of the pair-pair correlations with δ ,⁴³ indicating a superconducting phase as soon as the Mott insulator is doped, in the case of a finite t' , the FN results could be compatible with a finite critical doping, below which the system is not superconducting. This outcome is in agreement with earlier Monte Carlo calculations done by one of us,⁴⁴ where it was suggested that the extended t - J model with hoppings and super-exchange interactions derived from structural data of the La_2CuO_4 compound could explain the main experimental features of high-temperature superconducting materials, with a finite critical doping for the onset of electron pairing.

Remarkably, from $\delta \sim 0.1$ to $\delta \sim 0.4$ there are huge size effects. Though, for $\delta \sim 0.3$, small clusters, e.g., $L = 98$, indicate stronger pairing correlations than the

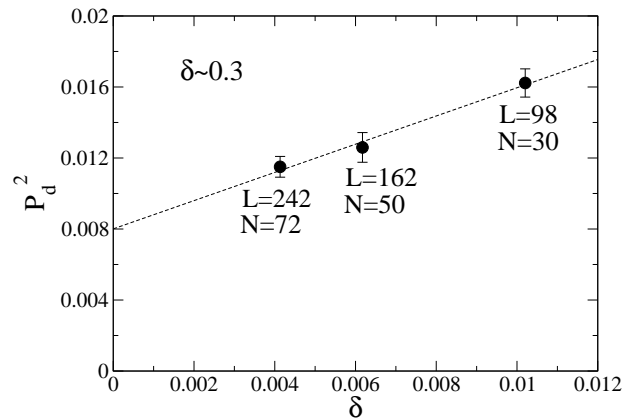


FIG. 9: Size scaling of the Pair-pair correlations at the maximum distance for t - t' - J model with $J/t = 0.2$ and $t'/t = -0.2$ at $\delta \sim 0.3$.

pure t - J model without t' , larger clusters point out a large reduction of P_d^2 . Nonetheless, we have a rather clear evidence that for $\delta \sim 0.3$ there is a finite superconducting order parameter in the thermodynamic limit, see Fig. 9. This strong reduction of the superconducting correlations is a very interesting effect, demonstrating that the superconducting wave function (even if supplemented by magnetic order) deteriorates its accuracy by increasing the value of t' , that could eventually stabilize competing phases with modulation in the charge distribution and/or a magnetic flux through the plaquettes.⁴⁵ However, for $t'/t = -0.2$, the homogenous variational ansatz (2) provides a lower energy when compared to the one used in Ref. 45.⁴⁶ At present, the most accurate FN calculations based on the lowest-energy variational ansatz, do not show any tendency towards charge inhomogeneities for $\delta \lesssim 0.4$. This outcome is important because in principle the FN approach can spontaneously induce charge-density wave modulations in the ground state, even when the variational wave function before the FN projection is translationally invariant.¹²

IV. CONCLUSION

In this paper, we considered the magnetic and superconducting properties of the t - t' - J model within VMC and FN approaches. We showed that for $t' = 0$ the ground-state properties can be accurately reproduced by a state containing both electron pairing and suitable magnetic correlations, namely a magnetic order parameter in the mean-field Hamiltonian that defines the fermionic determinant and a spin Jastrow factor for describing the spin fluctuations. In this case, we obtain a rather large magnetic phase, with a critical doping that slightly depends upon the super-exchange coupling J , i.e., $\delta_c = 0.10 \pm 0.01$ and $\delta_c = 0.13 \pm 0.02$ for $J/t = 0.2$ and $J/t = 0.4$, respectively. The superconducting correlations show a dome-like behavior and vanish when the

Mott insulator at half filling is approached. Interestingly, compared to the RMFT that predicts a quadratic behavior of the pair-pair correlations as a function of the doping δ , here we found that a linear behavior is more plausible.

Then, we also reported important modifications due to the presence of a finite ratio t'/t . The first effect of this further hopping term is to strongly suppress antiferromagnetic correlations at low doping, shifting the critical doping to 0.03 for $t'/t = -0.2$. This is a genuine effect of the FN method, since, within the pure variational approach, though the spin-spin correlations are suppressed with respect to the case of $t' = 0$, the values of the critical doping for these two cases are very similar. Most importantly, the presence of a finite value of the next-nearest-neighbor hopping has dramatic effects on the superconducting properties. At small doping, i.e., $\delta \lesssim 0.1$ there is a sizable suppression of the electronic pairing, possibly pointing toward a metallic phase in the slightly doped regime, as previously suggested by using improved Monte Carlo techniques.⁴⁴ Moreover, for $0.1 \lesssim \delta \lesssim 0.4$, though small lattices seem to indicate an increasing of superconductivity compared to the pure $t-J$ model, larger clusters show huge size effects that strongly renormalize the pairing correlations at large distance. However, for the value of t' considered in this work, we are rather con-

fident that superconducting off-diagonal long-range order takes place in a considerable hole region. In any case, the huge renormalization of the electronic pairing for $\delta \sim 0.3$, together with the fact that the FN results are very different from the VMC ones based on a wave function containing pairing (and magnetic order at low doping), suggests the possibility of the existence of a non-superconducting phase (with magnetic fluxes and/or charge order) that could be eventually stabilized by further increasing the ratio t'/t .

In conclusion, the main qualitative features of the cuprate phase diagram appear rather well reproduced by the $t-t'-J$ model with a sizable next-nearest-neighbor hopping. However, we do not find a sizable enhancement of the pairing correlations by increasing the ratio t'/t , that looks in contradiction with the empirical relation between t'/t and the value of T_c .²⁶ However, we have to remark that we only considered ground-state properties and we cannot evaluate T_c , whose relation with the pairing correlations may be highly non trivial, especially in a strongly-correlated system, like the $t-J$ model. This issue certainly deserves further work.

We thank useful discussions with S. Bieri, M. Capello, and D. Poilblanc. This research has been supported by PRIN-COFIN 2005 and CNR-INFM.

-
- ¹ J. Bardeen, L.N. Cooper, and J.R. Schrieffer, Phys. Rev. **108**, 1175 (1957).
- ² A. Lanzara, P.V. Bogdanov, X.J. Zhou, S.A. Kellar, D.L. Feng, E.D. Lu, T. Yoshida, H. Eisaki, A. Fujimori, K. Kishio, J.-I. Shimoyama, T. Noda, S. Uchida, Z. Hussain, and Z.-X. Shen, Nature (London) **412**, 510 (2001).
- ³ G.-H. Gweon, S.Y. Zhou, M.C. Watson, T. Sasagawa, H. Takagi, and A. Lanzara, Phys. Rev. Lett. **97**, 227001 (2006).
- ⁴ S. Sorella, G.B. Martins, F. Becca, C. Gazza, L. Capriotti, A. Parola, and E. Dagotto, Phys. Rev. Lett. **88**, 117002 (2002).
- ⁵ Th. Maier, M. Jarrell, T. Pruschke, and M.H. Hettler, Rev. Mod. Phys. **77**, 1027 (2005).
- ⁶ D. Eichenberger and D. Baeriswyl, arXiv:0708.2795 (unpublished).
- ⁷ P.W. Anderson, Science **235**, 1196 (1987).
- ⁸ F.C. Zhang and T.M. Rice, Phys. Rev. B **37**, 3759 (1988).
- ⁹ C. Gros, Phys. Rev. B **38**, 931 (1988).
- ¹⁰ S.R. White and D.J. Scalapino, Phys. Rev. Lett. **80**, 1272 (1998).
- ¹¹ S.R. White and D.J. Scalapino, Phys. Rev. Lett. **81**, 3227 (1998).
- ¹² F. Becca, L. Capriotti, and S. Sorella, Phys. Rev. Lett. **87**, 167005 (2001).
- ¹³ P.W. Anderson, P.A. Lee, M. Randeria, T.M. Rice, N. Trivedi, and F.C. Zhang, J. Phys.: Condensed Matter **24**, R755 (2004).
- ¹⁴ For a recent review on the RMFT and variational Monte Carlo based on the RVB wave function, see for instance, B. Edegger, V.N. Muthukumar, and C. Gros, to be published in Advances in Physics.
- ¹⁵ C. Gros, Phys. Rev. B **42**, 6835 (1990).
- ¹⁶ D.A. Ivanov, Phys. Rev. B **70**, 104503 (2004).
- ¹⁷ E. Manousakis, Rev. Mod. Phys. **63**, 1 (1991).
- ¹⁸ F. Franjic and S. Sorella, Prog. Theor. Phys. **97**, 399 (1997).
- ¹⁹ F. Becca, M. Capone, and S. Sorella, Phys. Rev. B **62**, 12700 (2000).
- ²⁰ J.P. Bouchaud, A. Georges, and C. Lhuillier, J. de Physique **49**, 553 (1988).
- ²¹ M. Lugas, L. Spanu, F. Becca, and S. Sorella, Phys. Rev. B **74**, 165122 (2006).
- ²² Y. Sidis, C. Ulrich, P. Bourges, C. Bernhard, C. Niedermayer, L.P. Regnault, N.H. Andersen, and B. Keimer, Phys. Rev. Lett. **86**, 4100 (2001).
- ²³ J.A. Hodges, Y. Sidis, P. Bourges, I. Mirebeau, M. Hennenion, and X. Chaud, Phys. Rev. B **66**, 020501(R) (2002).
- ²⁴ H.A. Mook, P. Dai, S.M. Hayden, A. Hiess, J.W. Lynn, S.-H. Lee, and F. Dogan, Phys. Rev. B **66**, 144513 (2002).
- ²⁵ E. Dagotto, Science **309**, 257 (2005).
- ²⁶ E. Pavarini, I. Dasgupta, T. Saha-Dasgupta, O. Jepsen, and O.K. Andersen, Phys. Rev. Lett. **87**, 047003 (2001).
- ²⁷ K. Tanaka, T. Yoshida, A. Fujimori, D.H. Lu, Z.-X. Shen, X.-J. Zhou, H. Eisaki, Z. Hussain, S. Uchida, Y. Aiura, K. Ono, T. Sugaya, T. Mizuno, and I. Terasaki, Phys. Rev. B **70**, 092503 (2004).
- ²⁸ T. Tohyama and S. Maekawa, Phys. Rev. B **49**, 3596 (1994).
- ²⁹ S.R. White and D.J. Scalapino, Phys. Rev. B **60**, 753(R) (1999).
- ³⁰ A. Himeda, T. Kato, and M. Ogata, Phys. Rev. Lett. **88**, 117001(2002).
- ³¹ C.T. Shih, T.K. Lee, R. Eder, C.-Y. Mou, and Y.C. Chen,

- Phys. Rev. Lett. **92**, 227002 (2004).
- ³² C.T. Shih, Y.C. Chen, C.P. Chou, and T.K. Lee, Phys. Rev. B **70**, 220502(R) (2004).
- ³³ M. Raczkowski, R. Fresard, and A.M. Oles, Phys. Rev. B **73**, 174525 (2006).
- ³⁴ S. Sorella, Phys. Rev. B **71**, 241103 (2005); S. Yunoki and S. Sorella, Phys. Rev. B **74**, 014408 (2006).
- ³⁵ D.F.B. ten Haaf, H.J.M. van Bemmelen, J.M.J. van Leeuwen, W. van Saarloos, and D.M. Ceperley, Phys. Rev. B **51**, 13039 (1995).
- ³⁶ N. Trivedi and D.M. Ceperley, Phys. Rev. B **41**, 4552 (1990).
- ³⁷ M. Calandra and S. Sorella, Phys. Rev. B **57**, 11446 (1998).
- ³⁸ D.M. Ceperley and B.J. Alder, Phys. Rev. Lett. **45**, 566 (1980).
- ³⁹ V.J. Emery, S.A. Kivelson, and H.Q. Lin, Phys. Rev. Lett. **64**, 475 (1990).
- ⁴⁰ A. Macridin, M. Jarrell, and Th. Maier, Phys. Rev. B **74**, 085104 (2006).
- ⁴¹ N. Furukawa and M. Imada, J. Phys. Soc. Jpn. **61**, 3331 (1992).
- ⁴² K. Yamada, C.H. Lee, K. Kurahashi, J. Wada, S. Wakimoto, S. Ueki, H. Kimura, Y. Endoh, S. Hosoya, G. Shirane, R.J. Birgeneau, M. Greven, M.A. Kastner, and Y.J. Kim, Phys. Rev. B **57**, 6165 (1998).
- ⁴³ In contrast to RMFT, that predicts a quadratic behavior of the pair-pair correlations, the variational results show that these correlations have instead a linear behavior with δ in the underdoped regime, even in the simplest case without Jastrow term. See for instance, S. Bieri and D. Ivanov, Phys. Rev. B **75**, 035104 (2007).
- ⁴⁴ V.I. Anisimov, M.A. Korotin, I.A. Nekrasov, Z.V. Pchelkina, and S. Sorella, Phys. Rev. B **66**, 100502 (2002).
- ⁴⁵ M. Raczkowski, M. Capello, D. Poilblanc, R. Fresard, and A.M. Oles, arXiv:0708.0788 (unpublished).
- ⁴⁶ We thank M. Capello for providing us with the variational energies of the wave function used in Ref. 45.